WOOD RESEARCH doi.org/10.37763/wr.1336-4561/66.4.643656
e-ISSN 2729-8906
66(4): 2021 643-656 pp.

EFFECTS OF STAND DENSITY ON TURPENTINE TERPENE COMPONENTS AND RESIN DUCT MORPHOLOGICAL STRUCTURE OF *PINUS MASSONIANA*

JIANHUA LYU, CHENG GUAN, XIANWEI LI, MING CHEN
SICHUAN AGRICULTURAL UNIVERSITY
CHINA

(RECEIVED OCTOBER 2020)

ABSTRACT

The influence of stand density on the resin duct morphological structure and terpene components of *Pinus massoniana* were studied. The resin duct morphological characteristics and the relative content of the terpene components were investigated by microscopy and gas chromatography-mass spectroscopy, respectively. The experimental results revealed that there was a specific correlation between the stand density and resin duct area, resin duct diameter, and the relative contents of main terpene components in the turpentine extracts. Additionally, the relative contents of *β*-pinene and (+)-camphene were positively correlated with stand density, with correlation coefficients of 0.8208 and 0.5539, respectively. In contrast, the relative contents of (+)-longifolene and (+)-longicyclene were negatively correlated with stand density, with correlation coefficients of -0.5750 and -0.7726, respectively, and *α*-pinene, *β*-caryophyllene, and (+)-*α*-longipinene had no correlation with stand density. The relative content of (+)-*α*-pinene was negatively correlated with the relative contents of both (+)-longifolene and (+)-longicyclene, with correlation coefficients of -0.8770 and -0.8914, respectively. There were positive correlations between the relative contents of (+)-longifolene and (+)-longicyclene with correlation coefficient of 0.9718, (+)-longifolene and (+)-*α*-longipinene with correlation coefficient of 0.8399, *β*-caryophyllene and (+)-*α*-longipinene with correlation coefficient of 0.9360, and (+)-longicyclene and (+)-*α*-longipinene with correlation coefficient of 0.8626.

KEYWORDS: *Pinus massoniana*, stand density, terpene components, resin duct morphological structure.

INTRODUCTION

Pinus massoniana Lamb., also known as Masson pine, belongs to the family Pinaceae Lindl., Pinus Linn., and is widely available in Central and Southern China. *Pinus massoniana*

is an important resin-producing tree species in China; more than 90% of the pine resin in China is tapped from *P. massoniana* (Lai et al. 2020).

A resin duct is a typical self-protective structure of Pinaceae plants and is the first line of defense against insects and pathogens (Roberds et al. 2003, King et al. 2011). Pine oleoresin secreted by the resin duct is a mixture of terpenoids, and is a transparent and colorless mucus. Pine oleoresin is the leading secondary metabolite of pine, and it can be made into rosin, turpentine, and other valuable industrial raw materials using heat and distillation to remove any impurities (Rodrigues-Corrêa et al. 2012).

Most of the research literature focuses on forest resource management, genetic breeding, and pest control (Song et al. 2005, Zeng and Tang 2012, Ali et al. 2019, Ni et al. 2019). Additionally, few of the published research discusses the relationship between the stand density, the microstructure or macrostructure of wood, and the resin yield of trees (Giagli et al. 2019, Lyu et al. 2020).

Some studies show that the chemical components of resin, the resin flow rate, the number and density of resin ducts, and other defensive characteristics of many coniferous trees are controlled by their heredity, which are the stable genetic characteristics of the trees (Roberds et al. 2003, Franceschi et al. 2005, King et al. 2011, Moreira et al. 2012).

Resin ducts and resin cells are two characteristic structures commonly found in pine needles and trunks (Berryman 1972). Wu and Hu (1995) studied the relationship between the resin duct morphological structure, resin yield, and secretion of the tree *Pinus tabulaeformis*, then clarified the mechanism for resin synthesis and secretion. Zhu and Huang (2002) found a significant positive correlation between the number of resin ducts and the resin yield of *P. massoniana*. In addition, the resin yield capacity of pine is related to the resin duct diameter: a larger resin duct diameter results in a higher flow velocity and flow amount (Phillips and Croteau 1999). Mu et al. (2012) found that the number of resin ducts and resin cells in high resin-yield trees was higher than that in low resin-yield trees, which can be used as a noticeable and valuable index for early screenings of the high resin-yielding capacity of *Pinus kesiya* var. *langbianensis* trees. A similar conclusion was reached by Lombardero et al. (2000) in which the resin yield of *Pinus yunnanensis* is closely related to the number of resin ducts in the needles, the phloem and xylem, and the area of resin ducts in the phloem. However, analyzing the factors affecting the resin yield of 79 high-yielding *P. massoniana* trees from different regions shows that the resin yield of *P. massoniana* has little relationship with the diameter and number of sapwood resin ducts and instead shows that it is related to the area of the resin ducts (Moghaddama and Farhadib 2015). Other research focused on *P. massoniana* clones has similar conclusions (Liu et al. 2013). Others have found a remarkable difference in the resin yield of *P. massoniana* with different densities. Increasing the stand density results in an increase in the resin yield per unit area of *P. massoniana* but additionally results in a decrease in the average annual yield per plant. However, increasing the stand density to a certain extent results in a decrease in the resin yield per unit area (Rodríguez-García et al. 2014, Neis et al. 2018).

The aims of this paper are: *(a)* to investigate the relationship between the stand density and the resin duct morphological structure of *P. massoniana*; and *(b)* the relationship between the stand density and the terpene components in turpentine extracts of *P. massoniana*.

MATERIAL AND METHODS

Materials

The turpentine extracts were collected from the sample trees of *Pinus massoniana* plantation, located in Damaoping area of Pingchang County (Bazhong, China) at an altitude of approximately 740 m. Four plots with an area of approximately 600 m^2 were delineated using a round quadrat method. The stand density of each sample plot was 833 plants/hm^2, 1000 plants/hm^2, 1167 plants/hm^2, and 1333 plants/hm^2, and each plot was labeled Group A, B, C, and D, respectively. Five *P. massoniana* trees with diameter at breast height (DBH) of 20 to 35 cm were randomly selected from each group and were harvested for resin at 1.2 m above the ground surface. The resin from each group was collected separately, packed in vacuum bags, and stored with no access to light. After the completion of resin tapping, all the sample trees were cut down, and the discs of corresponding resin tapping areas were collected for wood anatomical experiments. Finally, the turpentine was extracted via a steam distillation method in the laboratory.

Methods

Resin duct morphological characteristics determination experiment

Each disc was cut into five samples (10 × 10 × 10 mm) with an electric jigsaw. Samples were softened in distilled water for 6 h and then sliced into 30-μm sections by a sliding microtome on the cross-section, radial section, and tangential section. The sections were stained with 0.1% safranine for 1 to 2 min, dehydrated in graded alcohols (30%, 50%, 75%, 95%, and 100%) 5 min each, and cleaned for 5 min in fresh xylene.

The wood anatomical characteristics were determined via image analysis on histological cuts using a microscope (Leica DM500; Leica Microsystems, Wetzlar, Germany) at a magnification of 40x to 400x and analyzed with Leica Application Suite (LAS) EZ software (Leica Microsystems, Version 4.2.0, Wetzlar, Germany) (Fig. 1).

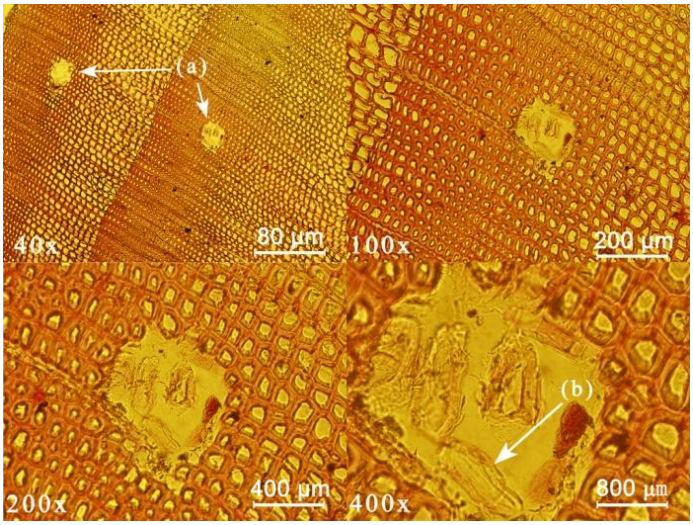

Fig. 1: Cross-section of a wood sample of P. massoniana: (a) resin ducts and (b) resin cells.

The following characteristics were measured: resin duct area (μm^2), resin duct density (cells/mm^2), the total area of resin duct per unit area ($\mu m^2/mm^2$), the length-width ratio of the resin cell, resin duct diameter (μm), and the ratio of wall-to-cavity of the resin cell.

Relative content of terpenes in turpentine extracts determination experiment

The terpenes components in the turpentine extracts were analyzed by a gas chromatograph-mass spectrometer (GCMS-QP2010 Plus; Shimadzu, Tokyo, Japan). Helium was used as the carrier gas with a flow rate of 1.2 $mL \cdot min^{-1}$. The gas chromatograph (GC) oven temperature was programmed at 50°C (held 2 min), raised to 120°C (held 2 min) at $10°C \cdot min^{-1}$, raised to 260°C at $5°C \cdot min^{-1}$, and subsequently to 290°C (held 15 min) at $10°C \cdot min^{-1}$. The injector temperature was set at 220°C, and the GC split ratio was adjusted to 10 : 1. A sample of 1.0 μL was injected using the splitless mode after being dissolved into n-hexane, and the mass conditions were as follows: electron impact ionization was employed with a collision energy of 70 eV, and the mass spectrometer ion source was maintained at 200°C, full scan mode in the m/z range 1250 with a 0.50 s/scan velocity. The relative concentration (%) was determined by integrating all peaks obtained in the total ion chromatogram (TIC) mode. The terpene components were identified via comparison of the mass spectra with the NIST08 library (NIST, Version 2.0, Gaithersburg, MD, USA).

RESULTS AND DISCUSSION

Relationship between stand density and resin duct morphological characteristics

The programming language R (R Foundation for Statistical Computing, Version 3.6.3, Vienna, Austria) was used to analyze the correlation coefficient and linear regression between the stand density and the resin duct morphological characteristics. The results from the analysis of stand density with each of the following are shown in Fig. 2, respectively: resin duct area, resin duct diameter, resin duct density, the total area of resin duct per unit area, the length-width ratio of the resin cell, and the ratio of wall-to-cavity of the resin cell.

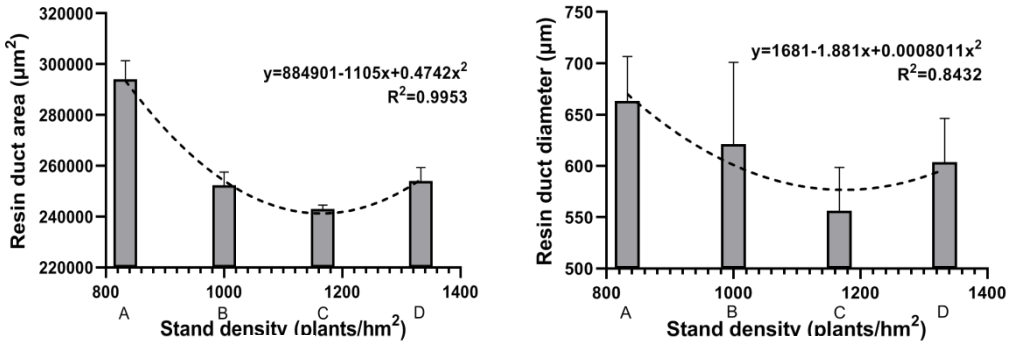

(a) **(b)**

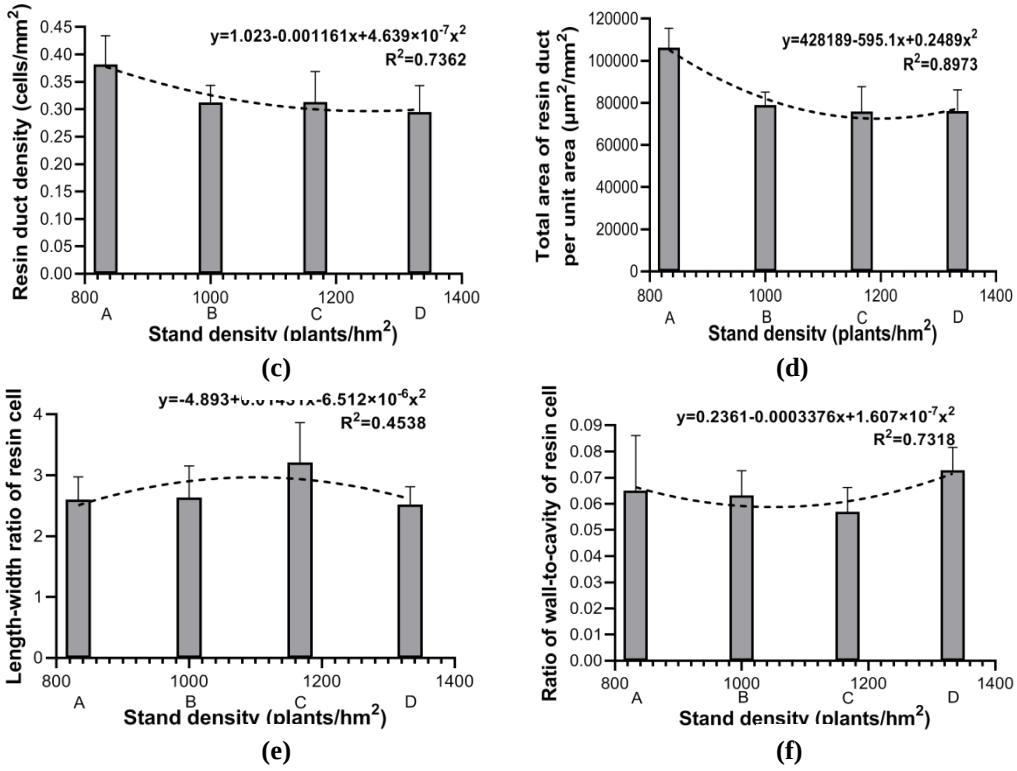

Fig. 2: Linear regression of stand density and resin ducts morphological characteristics: (a) stand density and resin duct area; (b) stand density and resin duct diameter; (c) stand density and resin duct density; (d) stand density and total area of resin duct per unit area; (e) stand density and length-width ratio of resin cell; (f) stand density and ratio of wall-to-cavity of resin cell.

Figs. 2a,b show that increasing the stand density resulted in a significant decrease in the resin duct area at a level of p = 0.05. This decrease in the resin duct area slowed after the stand density reached a level of 1167 plants/hm^2. The direct correlation between the resin duct area and the resin duct diameter showed that the changing trend of the resin duct diameter with the stand density was similar to that of the resin duct area; however, the standard deviation value for the latter was higher due to the noticeable difference within the group. When the stand density was 833 plants/hm^2, the resin duct area and resin duct diameter reached the maximum. Because of the limited environmental conditions of the sample plot, the sampling range of stand density could not be expanded, so it was impossible to determine whether the changing trend of resin duct area and resin duct diameter would rise or becomes slow. Based on relevant research reports by Lombardero et al. (2000) and Liu et al. (2013), it can be deduced that the maximum resin yield was in this study gradient at 833 plants/hm^2. Meanwhile, increasing stand density resulted in a decrease in the resin duct area and resin duct diameter, leading to the decline of resin yield per plant. This showed similar results to other studies (Rodríguez-García. 2014).

As shown in Fig. 2c,d the resin duct density and the total area of resin duct per unit area were negatively correlated with the stand density in the range of 833 to 1333 plants/hm^2 with small correlation coefficient R^2 value.

From Fig. 2e,f the standard deviation of the length-width ratio of the resin cell and the ratio of wall-to-cavity of the resin cell in the range of 833 to 1333 plants/hm^2 was too high. Additionally, the R^2 values obtained of the fitting curve was too low, so the fitting curves have no reference value. Therefore, the correlation between the stand density and the length-width ratio of the resin cell, and between stand density and ratio of wall-to-cavity of resin cell are not significant in the range of 833 to 1333 plants/hm^2.

Relationship between stand density and terpene components in turpentine extracts

Quantification was determined *via* percentage peak area calculations using gas chromatography-flame ionization detector (GC-FID). The chromatographic peaks were preliminarily identified using an automatic search of the National Institute of Standards and Technology (NIST) gas chromatograph-mass spectrometry (GC/MS) library. The obtained mass spectra were then compared with those reported in previous literature (Adams 2007, Ioannou et al. 2014, Lyu et al. 2018). The chemical compounds were analyzed qualitatively using the relative reservation index and *via* peak area normalization measurements. The total ion chromatograms (TIC) of the turpentine terpene components in stand density Groups A, B, C, and D are shown in Fig. 3.

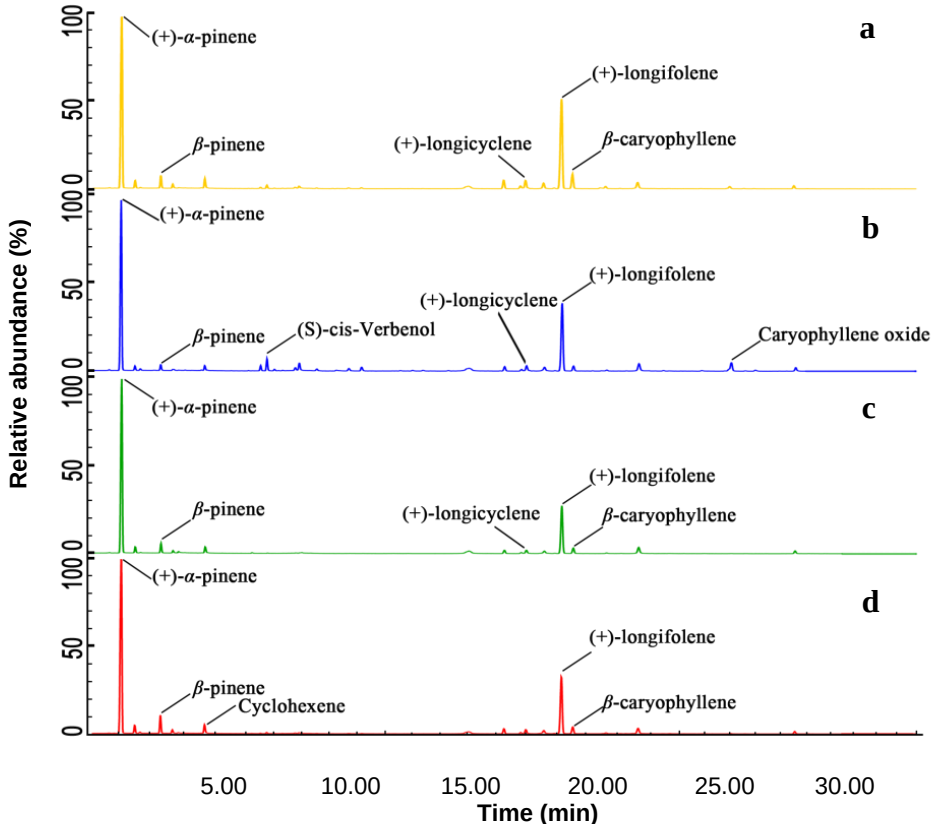

Fig. 3: Ion chromatogram of terpene components extracted from the turpentine extracts of Pinus massoniana plantations with different stand densities: (a) Group A with stand density 833 plants/hm^2; (b) Group B with stand density 1000 plants/hm^2; (c) Group C with stand density 1167 plants/hm^2; (d) Group D with stand density 1333 plants/hm^2.

The results of the relative content analysis showed that the content of (+)-*α*-pinene and (+)-longifolene were the first and second highest, which occupied 46.25% to 58.52% and 21.10% to 30.14% of total terpenes in turpentine extracts, respectively, and followed by *β*-caryophyllene in Groups A and C, in which its content was 4.12% and 3.55%, respectively. In group B, caryophyllen oxide ranked third in relative content with 3.56%, and in Group D, *β*-pinene ranked third in relative content with 4.42%. The top five relative contents of each group are marked on the graph; however, Group B shows six terpenes because the relative contents of *β*-pinene and (+)-longicyclene in Group B were both 1.86%. Other studies have shown partially similar results: (+)-*α*-pinene was also the dominant compound ranging from 34.99% to 43.60%, followed by *β*-pinene ranging from 15.29% to 29.40%, but (+)-longifolene only ranked fourth ranging from 4.39% to 6.78% (Tümen and Reunanen 2010).

Additionally, R was used to analyze the correlation coefficient and the linear regression between the stand density and relative content of the main terpene components in turpentine extracts. The results of stand density and (+)-*α*-pinene, (+)-longifolene, *β*-pinene, *β*-caryophyllene, cyclohexene, (+)-camphene, (+)-longicyclene, (+)-*α*-longipinene, and 7-methyl-3-methyleneocta-1,6-diene are shown in Fig. 4a through Fig. 4i.

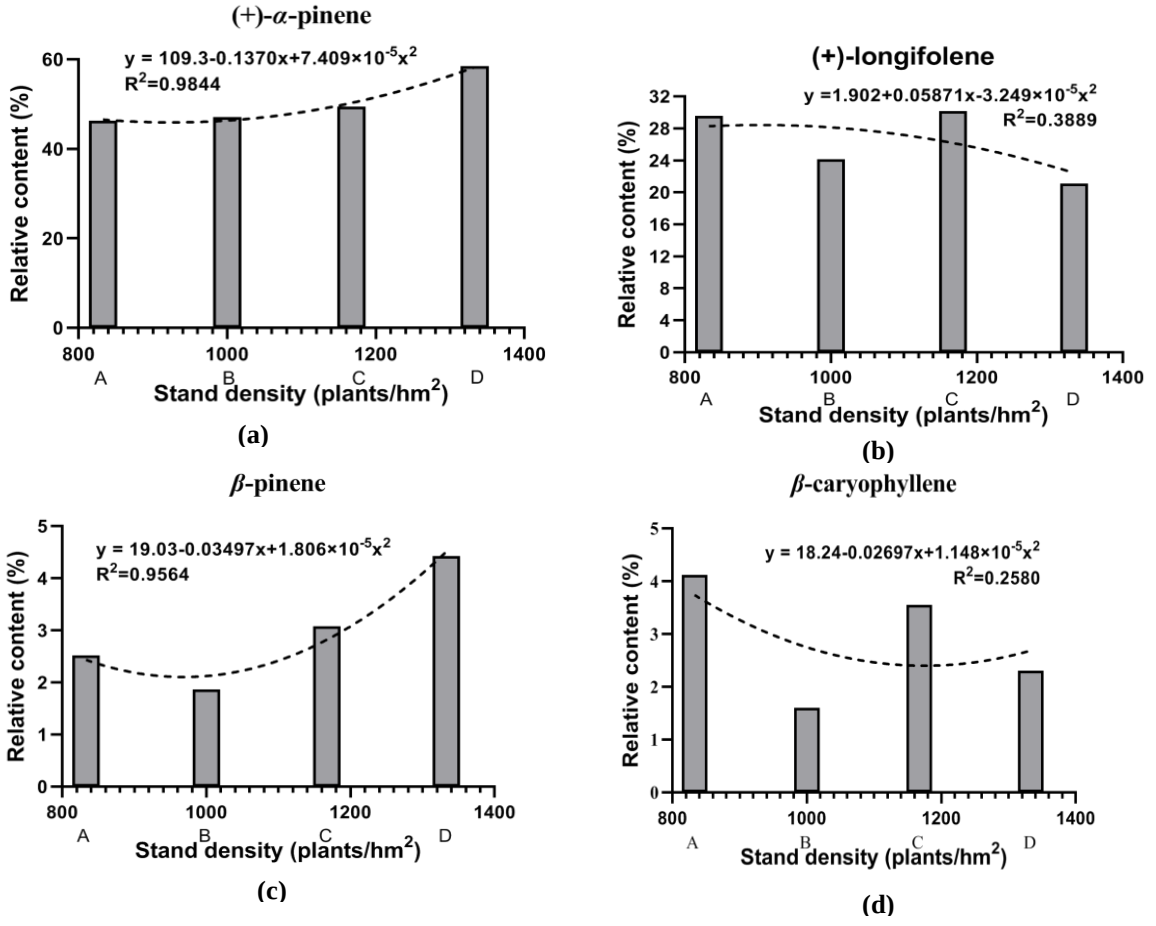

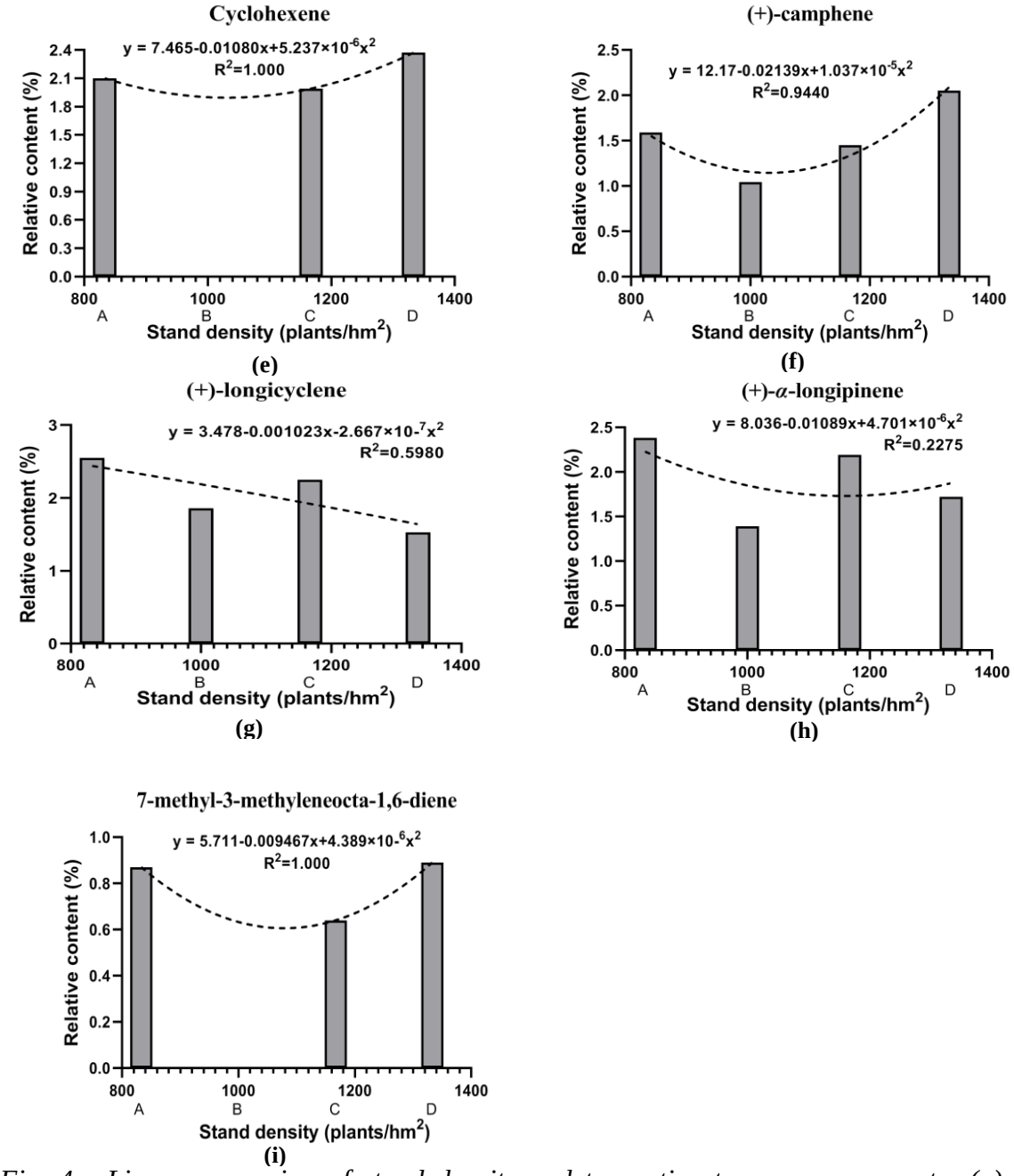

Fig. 4: Linear regression of stand density and turpentine terpene components: (a) stand density and (+)-α-pinene; (b) stand density and (+)-longifolene; (c) stand density and β-pinene; (d) stand density and β-caryophyllene; (e) stand density and cyclohexene; (f) stand density and (+)-camphene; (g) stand density and (+)-longicyclene; (h) stand density and (+)-α-longipinene; (i) stand density and 7-methyl-3-methyleneocta-1,6-diene.

According to Fig. 4a, there was a positive correlation between the relative content of *α*-pinene in the turpentine extracts with a stand density in the range of 833 to 1333 plants/hm^2. The relative content of *α*-pinene at the stand density of 1333 plants/hm^2 was positive at a p = 0.05 level when compared with the relative content at the stand density of 833 plants/hm^2. According to Fig. 4b, the relative content of (+)-longifolene at 1000 and 1333 plants/hm^2 showed significance at p = 0.05 and 0.01 level, respectively. According to

Fig. 4c, there was a positive correlation between the relative content of *β*-pinene in turpentine extracts and stand density in the range of 1000 to 1333 plants/hm^2 with R^2 = 0.9564. The *β*-pinene relative content at stand density of 1000 plants/hm^2 showed significance at p = 0.05 level, and at stand density of 1333 plants/hm^2 extremely significant at p = 0.01 level. According to Fig. 4d, the *β*-caryophyllene relative contents at stand densities of 1000 and 1333 plants/hm^2 both showed extreme significance at p = 0.01 level. According to Fig. 4e, the cyclohexene relative content in turpentine extracts at the stand density of 1333 plants/hm^2 showed significance at a p = 0.05 level. However, due to the absence of cyclohexene in Group B, although the R^2 value of the fitting curve generated by polynomial curve fitting was ideal, the positive correlation between cyclohexene and stand density in the range of 833 to 1333 plants/hm^2 could not be determined. According to Fig. 4f, there was a positive correlation between the (+)-camphene relative content and stand density in the range of 1000 to 1333 plants/hm^2. The relative content of (+)-camphene at a stand density of 1000 plants/hm^2 showed extreme significance at a p = 0.01 level, and the relative content at the stand density of 1333 plants/hm^2 showed significance at a p = 0.05 level. According to Fig. 4g, the relative contents of (+)-longicyclene at 1000 and 1333 plants/hm^2 showed extreme significance at a p = 0.01 level, but no correlation conclusion could be drawn between the relative content of (+)-longicyclene and stand density in the range of 833 to 1333 plants/hm^2, and the fitting curve here was approximate to a straight line. According to Fig. 4h, the relative content of (+)-*α*-longipinene at 1000 and 1333 plants/hm^2 showed significance at p = 0.01 and 0.05 level, respectively. According to Fig. 4(i), the relative content of 7-methyl-3-methyleneocta-1,6-diene in the turpentine extracts at a stand density of 1167 plants/hm^2 showed extreme significant correlation at a p = 0.01 level. However, it could not be determined that there was any correlation between 7-methyl-3-methyleneocta-1,6-diene and stand density in the range of 833 to 1333 plants/hm^2 because of the missing values in Group B. The reason may be due to the instability of many substances in turpentine extracts, some components in the turpentine extracts will change in the structure under conditions where there is light; additionally, as the isomer of α-pinene, β-pinene will change into D-α-pinene or L-α-pinene under the action of the external physical environment, to a certain extent. Some α-pinene will produce α-pinene oxide through an oxidation-reduction reaction in air, and (+)-longifolene will transform into (+)-longicyclene in the presence of oxidants (Wilbon et al. 2013).

Correlation analysis of terpene components in turpentine extracts

Due to the missing values of cyclohexene and 7-methyl-3-methyleneocta-1,6-diene in the turpentine extracts of Group B, the two sets of data cannot be used for multiple comparisons, which affects the results of the comparisons. Therefore, cyclohexene and 7-methyl-3-methyleneocta-1,6-diene were excluded from the terpene components of turpentine extracts in the multiple comparisons.

The Pearson multiple comparison method was used *via* the programming language R to compare the filtered data, and the scatter plot matrix method was used to establish the matrix. Based on the results of the two analyses, the correlation between the relative content of the primary terpene components in turpentine extracts were analyzed, and the correlation

analysis and curve fitting of the main selected terpene components were implemented.

The Pearson multiple comparison method was used to obtain the correlation matrix among the terpene components (Fig. 5). The results were as follows: for the relative contents of *α*-pinene and (+)-longifolene, *α*-pinene and (+)-longicyclene were significantly negatively correlated; for the relative contents of (+)-longifolene and (+)-longicyclene, (+)-longifolene and (+)-*α*-longipinene were significantly positively correlated; lastly, there was a significant positive correlation between *β*-caryophyllene and (+)-*α*-longipinene and between (+)-longicyclene and (+)-*α*-longipinene.

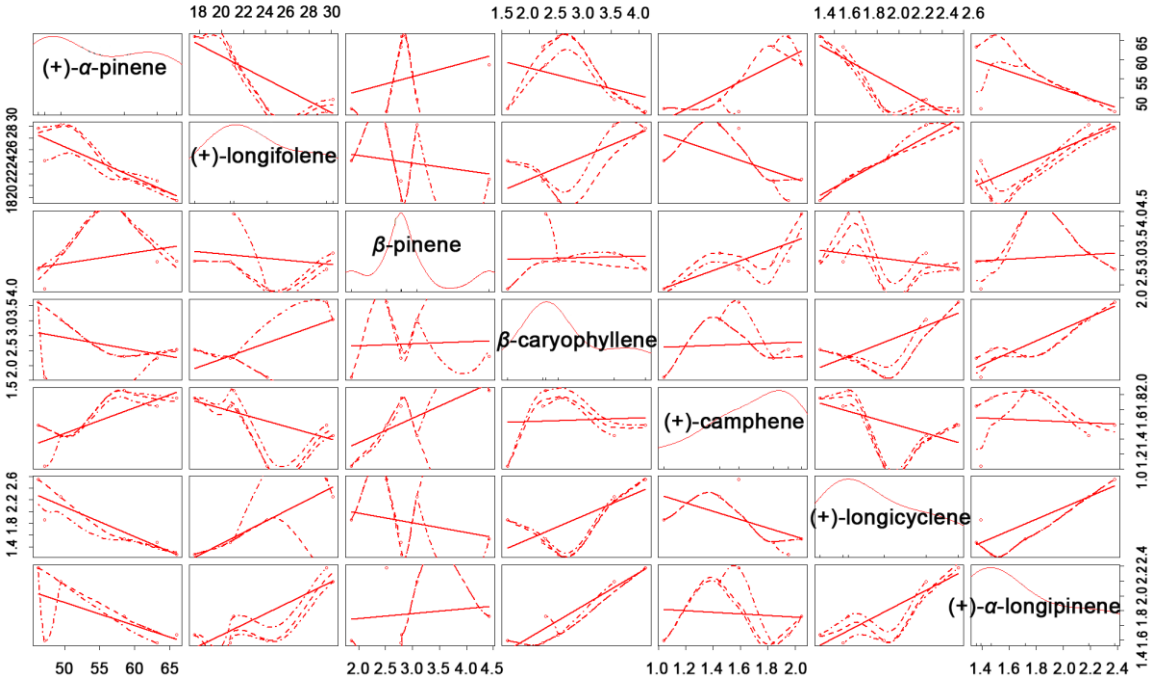

Fig. 5: Correlation matrix of the relative contents of main terpene components in turpentine extracts.

After summarizing and screening the results shown in Fig. 5, the possibly-related main terpene components were compared using analysis of variance method of the programming language R for a test on statistical significance. Then, the linear regression and binomial nonlinear regression were carried out by using the R software with function *lm()* which is used to fit linear models. Finally, the scatter diagram and regression model diagram were combined in Fig. 6.

As shown in Fig. 6, the correlation matrix and correlation analysis of six pairs of the main terpene components in the turpentine extracts have a good fitting effect, and all data showed that there was a significant correlation among them. There were linear correlations between *α*-pinene and (+)-longifolene, *α*-pinene and (+)-longicyclene, and (+)-longifolene and (+)-longicyclene, where the former two were the negative correlations and the latter was a positive correlation. In contrast, the curve correlation between (+)-longifolene and (+)-*α*-longipinene, *β*-caryophyllene and (+)-*α*-longipinene, and (+)-longicyclene and (+)-*α*-longipinene were more potent than the linear correlation. Additionally, all of them were positively correlated.

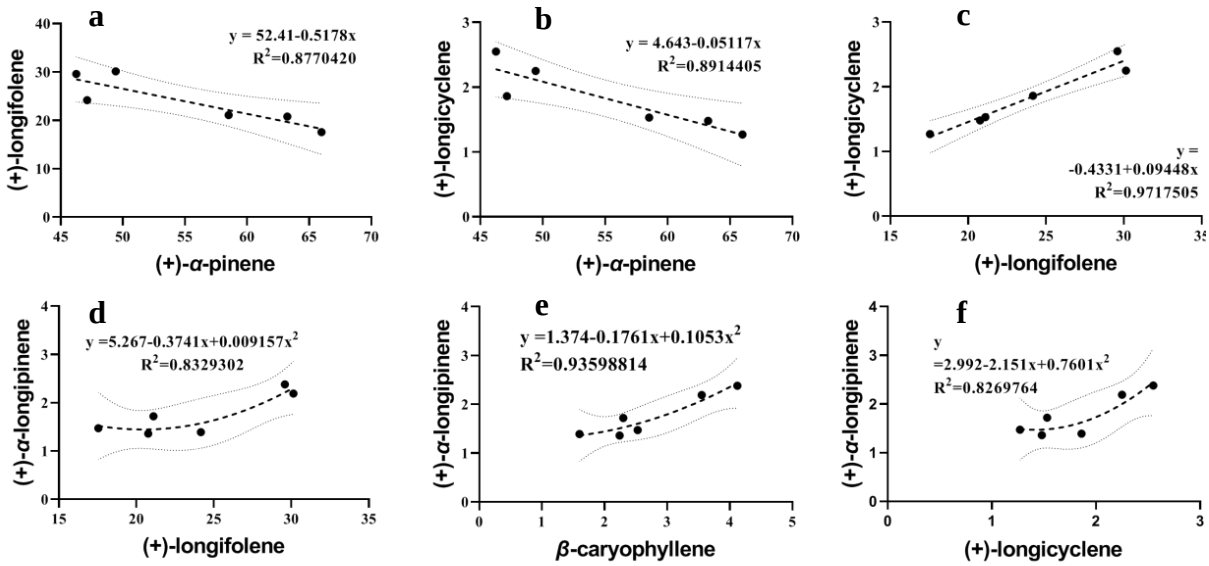

Fig. 6: Regression model between selected terpene components in turpentine extracts: (a) (+)-α-pinene and (+)-longifolene; (b) (+)-α-pinene and (+)-longicyclene; (c) (+)-longifolene and (+)-longicyclene; (d) (+)-longifolene and(+)-α-longipinene; (e) β-caryophyllene and (+)-α-longipinene; (f) (+)-longicyclene and (+)-α-longipinene.

Through the comparative analysis of the main terpene components in the turpentine extracts, it was found that some terpenes in the turpentine extracts showed a significant correlation. These correlations were a linear correlation or curvilinear correlation. The cause of the considerable relationship may be partly due to how some terpenes could be transformed into each other or were antagonistic to each other in chemical reactions. However, it may also be the stress of *P. massoniana* on the environment, which triggers gene regulation (Ren et al. 2008, Quan and Ding 2017).

CONCLUSIONS

(1) Under different stand densities, the resin duct morphological structure of *Pinus massoniana* followed a specific trend of change. The correlation factors of the resin duct morphological characteristics showed a similar trend of change. For example, the two elements with a higher correlation, i.e., the resin duct area and resin duct diameter, would be negatively correlated with the change of the stand density gradient in this study. When the stand density was 1167 plants/hm^2, the decrease in the resin duct area and resin duct diameter began to slow down. *(2)* The change of the stand density resulted in a change in the relative contents of the main terpene components in the *P. massoniana* turpentine. Some of the terpene components were positively correlated with the change of the stand density, such as *α*-pinene, *β*-pinene, and (+)-camphene, and some terpene components had no significant relationship with the evolution of the stand density, such as (+)-*α*-longipinene and *β*-caryophyllene. *(3)* Due to the absence of the two terpene components 7-methyl-3-methyleneocta-1,6-diene and cyclohexene, no relevant components were detected in Group B.

Therefore, it was impossible to determine the relationship between the changes of the two terpenes with the stand density. This may be due to the instability of many substances in the volatile oil of the turpentine extracts. A series of chemical reactions began when the resin flowed out of *P. massoniana* and was exposed to the air.

ACKNOWLEDGMENTS

The authors are grateful for the support of the Ministry of Education Humanities and Social Sciences Research Project of China (Grant No. 19YJC760009), the Key Research and Development Project of Sichuan Science and Technology Plan Projects (Grant No. 2020YFS0357), the Project of National Science & Technology Pillar Program during the 12th Five-year Plan Period (Grant No. 2011BAC09B05), German Government Loans for Sichuan Forestry Sustainable Management Project (Grant No. G1403083), the Project of Modern Design and Culture Research Center, Sichuan Key Research Base of Philosophy and Social Sciences (Grant No. MD18Z002), the Opening Foundation for Industrial Design Industry Research Center, Key Research Base of Humanities and Social Sciences, and the Sichuan Education Department (Grant No. GYSJ18-037).

REFERENCES

1. Adams, R.P., 2007: Identification of essential oils components by gas chromatography Quadrupole mass spectrometry. Allured Publishing Corporation, Carol Stream, IL, USA., 804 pp.
2. Ali, A., Dai, D., Akhtar, K., Teng, M., Yan, Z., Urbina-Cardona, N., Mullerova, J., Zhou, Z., 2019: Response of understory vegetation, tree regeneration, and soil quality to manipulated stand density in a *Pinus massoniana* plantation. Global Ecology and Conservation 20: e00775.
3. Berryman, A.A., 1972: Resistance of conifers to invasion by bark beetle-fungus associations. BioScience 22(10): 598-602.
4. Franceschi, V.R., Krokene, P., Christiansen, E., Krekling, T., 2005: Anatomical and chemical defenses of conifer bark against bark beetles and other pests. New Phytologist 167(2): 353-376.
5. Giagli, K., Vavrcik, H,. Fajstavr, M., Cerny, J., Novosadova, K., Martinik, A., 2019: Stand factors affecting the wood density of naturally regenerated young silver birch growing at the lower altitude of the Czech Republic region. Wood Research 64(6): 1011-1022.
6. Ioannou, E., Koutsaviti, A., Tzakou, O., Roussis, V., 2014: The genus *Pinus*: A comparative study on the needle essential oil composition of 46 pine species. Phytochemistry Reviews 13(4): 741-768.
7. King, J.N., Alfaro, R.I., Lopez, M.G., Van Akker, L., 2011: Resistance of Sitka spruce (*Picea sitchensis* (Bong.) Carr.) to white pine weevil (*Pissodes strobi* Peck): Characterizing the bark defense mechanisms of resistant populations. Forestry 84(1): 83-91.

8. Lai, M., Zhang, L., Lei, L., Liu, S., Jia, T., Yi, M., 2020: Inheritance of resin yield and main resin components in *Pinus elliottii* Engelm. at three locations in southern China. Industrial Crops and Products 144: 1-10.
9. Liu, Q., Zhou, Z., Fan, H., Liu, Y., 2013: Genetic variation and correlation among resin yield, growth, and morphologic traits of *Pinus massoniana*. Silvae Genetica 62(1-6): 38-43.
10. Lombardero, M.J., Ayres, M.P., Lorio Jr, P.L., Ruel, J.J., 2000: Environmental effects on constitutive and inducible resin defences of *Pinus taeda*. Ecology Letters 3(4): 329-339.
11. Lyu, J., Zhao, J., Xie, J., Li, X., Chen, M., 2018: Distribution and composition analysis of essential oils extracted from different parts of *Cupressus funebris* and *Juniperus chinensis*. BioResources 13(3): 5778-5792.
12. Lyu, J., Huang, W., Chen, M., Li, X., Zhong, S., Chen, S., Xie, J., 2020: Analysis of tracheid morphological characteristics, annual rings width and latewood rate of *Cupressus funebris* in relation to climate factors. Wood Research 65(4): 565-577.
13. Moghaddama, M., Farhadib, N., 2015: Influence of environmental and genetic factors on resin yield, essential oil content and chemical composition of *Ferula assa-foetida* L. populations. Journal of Applied Research on Medicinal and Aromatic Plants 2(3): 39-76.
14. Moreira, X., Alfaro, R.I., King, J.N., 2012: Constitutive defenses and damage in Sitka spruce progeny obtained from crosses between white pine weevil resistant and susceptible parents. Forestry 85(1): 87-97.
15. Mu, R., Wang, S., Pu, X., 2012: Anatomical comparison of the resin duct structure between the high and low resin yield trees of *Pinus kesiya* var. *langbianensis*. Journal of Forestry Engineering 26(2): 49-53.
16. Neis, F.A., de Costa, F., Füller, T.N., de Lima, J.C., da Silva Rodrigues-Corrêa, K.C., Fett, J.P., Fett-Neto, A.G., 2018: Biomass yield of resin in adult *Pinus elliottii* Engelm. trees is differentially regulated by environmental factors and biochemical effectors. Industrial Crops and Products 118(8): 20-25.
17. Ni, Z., Bai, T., Chen, Y., Huang, Y., Xu, L., 2019: Effects of parental genetic distance on offspring growth performance in *Pinus massoniana*: significance of parental-selection in a clonal seed orchard. Euphytica 215(12): 195.
18. Phillips, M.A., Croteau, R.B., 1999: Resin-based defenses in conifers. Trends in Plant Science 4(5): 184-190.
19. Quan, W., Ding, G., 2017: Dynamic of volatiles and endogenous hormones in *Pinus massoniana* needles under drought stress. Scientia Silvae Sinicae 53(4): 49-55.
20. Ren, Q., Hu, Y., Jin, Y., Deng, W., Li, Z., Yang, L., Nkoma, M.K., 2008: Rapid changes in induced non-volatile secondary metabolites in damaged *Pinus massoniana* Lamb. Frontiers of Forestry in China 3(3): 249–253.
21. Roberds, J.H., Strom, B.L., Hain, F.P., Gwaze, D.P., McKeand, S.E., Lott, L.H., 2003: Estimates of genetic parameters for oleoresin and growth traits in juvenile loblolly pine. Canadian Journal of Forest Research 33(12): 2469-2476.
22. Rodrigues-Corrêa, K.C.S., Lima, J.C., Fett-Neto, A.G., 2012: Pine oleoresin: tapping green chemicals, biofuels, food protection, and carbon sequestration from multipurpose trees. Food and Energy Security 1(2): 81-93.

23. Rodríguez-García, A., López, R., Martín, J.A., Pinillos, F., Gil, L., 2014: Resin yield in *Pinus pinaster* is related to tree dendrometry, stand density and tapping-induced systemic changes in xylem anatomy. Forest Ecology and Management 313(1): 47-54.
24. Song, J., Luo, Y., Shi, J., Yan, X., Chen, W., Jiang, A., 2005: Niche characteristics of boring insects within *Pinus massoniana* infected by *Bursaphelenchus xylophilus*. Journal of Beijing Forestry University 27(6): 108-111.
25. Tümen, İ., Reunanen, M., 2010: A comparative study on turpentine oils of oleoresins of *Pinus sylvestris* L. from three districts of Denizli. Records of Natural Products 4(4): 224-229.
26. Wilbon, P.A., Chu, F., Tang, C., 2013: Progress in renewable polymers from natural terpenes, terpenoids, and rosin. Macromolecular rapid communications 34(1): 8-37.
27. Wu, H., Hu, Z.H., 1995: The relation between the structure of resin ducts and the resin synthesis and mode of its elimination in *Pinus tabulaeformis*. Journal of Northwest University (Natural Science Edition) 25(5): 529-532.
28. Zeng, W, Tang, S., 2012: Modeling compatible single-tree aboveground biomass equations for masson pine (*Pinus massoniana*) in southern China. Journal of Forestry Research 23(4): 593-598.
29. Zhu, Q., Huang, Y., 2002: Regression analytical studies on the resin canal and resin-producing capacity of *Pinus massoniana*. Journal of Fujian Forestry Science and Technology 29(4): 15-16.

JIANHUA LYU, CHENG GUAN, XIANWEI LI, MING CHEN*
SICHUAN AGRICULTURAL UNIVERSITY
[1]COLLEGE OF FORESTRY
[2]WOOD INDUSTRY AND FURNITURE ENGINEERING KEY LABORATORY OF SICHUAN PROVINCIAL DEPARTMENT OF EDUCATION
CHENGDU, SICHUAN
CHINA
*Corresponding author: chenming@sicau.edu.cn